UDC 621.318.4

TECHNOLOGICAL TREND IN THE RECENT DEVELOPMENT OF SHUNT REACTOR

Yoshiaki Ikeda
Hironobu Naitô
Masaaki Abe

I. INTRODUCTION

Due to recent tendency of extremely high voltage, a long distance transmission line and underground cable, requirements of large capacity high voltage shunt reactors have been risen to compensate the condensive reactive power. Fuji Electric has concentrated its efforts actively in developing the shunt reactors, and since the first shunt reactor was delivered to a customer in 1964, Fuji Electric has manufactured 82 units 500 kV class, 6 units 400 kV class and many other shunt reactors and has accumulated the manufacturing experiences and technologies.

At the same time, Fuji Electric has proceeded developments of radially laminated core type shunt reactors which are very effective in reducing losses, noises and dimensions, toward a long period of time, and has confirmed the various excellent characteristics of radially laminated core type shunt reactors. And, through these studies and experiences, Fuji Electric has established the manufacturing technologies for shunt reactors using the radially laminated core as the standard type.

This paper introduces outline of Fuji Electric's recent technological trends and the manufacturing examples, centering around the test results of the 500 kV 80 MVA (bank power) radially laminated core type shunt reactor designed and manufactured based on the above mentioned technologies and recently delivered to the customer.

II. FUNDAMENTAL CONSTRUCTION AND FEATURES OF SHUNT REACTOR

A shunt reactor differs from a transformer in the facts that the shunt reactor uses one winding per phase and that the magnetic circuit has a gap. When classified based on the core in the winding, shunt reactors are classified into two types; gapped-core type and air-core type.

The gapped-core type is provided with a many number of gaps in the legs arranged in the winding, and *Fig. 1* shows a typical example.

On the other hand, the air-core type has no leg in the winding, and *Fig. 2* shows a typical example. The air-core type further increases the sum of the individual gaps of a

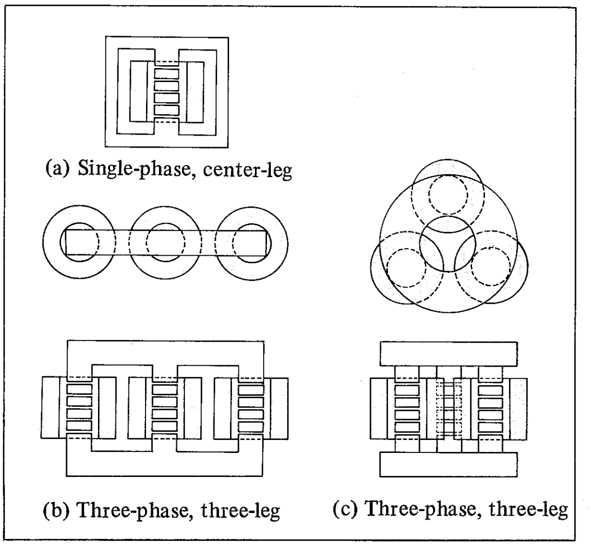

Fig. 1 Gapped-core type shunt reactor (typical example)

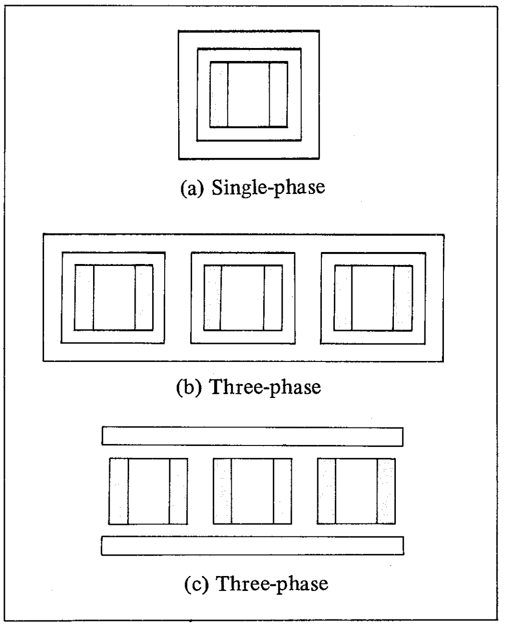

Fig. 2 Air-core type shunt reactor (typical example)

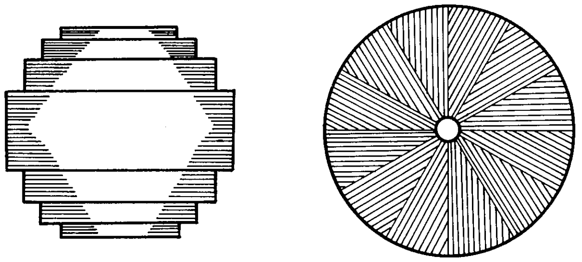

(a) Parallel laminated core (b) Radially laminated core

Fig. 3 Core constructions of gapped-core type shunt reactor

gapped-core type and makes a complete gap within the winding.

The gapped-core type is further classified into a parallel laminated core type and radially laminated core type by the core packet laminating methods. The parallel laminated core type laminates steel plates in parallel toward the same direction as shown in *Fig. 3-(a)*, and the radially laminated core type is constructed to a disc by laminating steel plates toward the radial direction as shown in *Fig. 3-(b)*.

Types of the shunt reactor are classified as shown below by the core constructions.

- Shunt reactor
  - Gapped-core type
    - Parallel laminated core type
    - Radially laminated core type
  - Air-core type

In anyone of these types, the fundamental characteristics of the reactor are expressed by the following equations:

$$B = \sqrt{2}\mu_0 \cdot \frac{N \cdot I}{G} \quad \cdots\cdots (1)$$

$$P = 2\pi f \cdot \frac{B^2}{2\mu_0} \cdot A \cdot G \quad \cdots\cdots (2)$$

$$L = \mu_0 \cdot \frac{A \cdot N^2}{G} \quad \cdots\cdots (3)$$

$$F = \frac{B^2}{2\mu_0} \cdot A = \frac{1}{2\pi f} \cdot \frac{P}{G} \quad \cdots\cdots (4)$$

where, P : Reactive power (VA)
B : Magnetic flux density (peak value) (tesla)
L : Reactance (H)
F : Magnetic attraction force (peak value)
f : Frequency (Hz)
μ_0 : Space permeability = $4\pi \times 10^{-7}$
A : Effective surface of air gap (m^2)
G : Total gap length (m)
N : Number of turns (turn)
I : Current (A)

In case of a gapped-core type, the magnetic flux density B of the space is enhanced because silicon steel plates having a far higher permeability than the space are arranged in the winding. Consequently, when the dimention is the same as an air-core type, the effective volume of space $A \cdot G$ reduces because the gap length of the gapped-core type is shorter than that of the air-core type. However, the reactive power can be increased two to three times as great as that of the air-core type in as much as the higher magnetic flux density B. Contrarily, when a gapped-core type shunt reactor is compared with an air-gap type having the same power, the former can be made in smaller in the dimensions and lighter in the weight.

Generally, as the power of a shunt reactor increases, the reactance reduces that much, and therefore, in case of a gapped-core type, the total gap length must be increased. For this reason, when using the gapped-core type for a large power reactor, many number of small gaps would be distributed to legs or a single gap length must be increased. The former requires to make extremely small split iron blocks and increases number of manufactured pieces, causing a problem in the manufacturing. In the latter case, leakage flux, in other words, so called fringing flux like a one shown in *Fig. 4* increases in proportion to length of the gap, causing eddy current losses to increase at the core packet and winding, and a local heating is resulted.

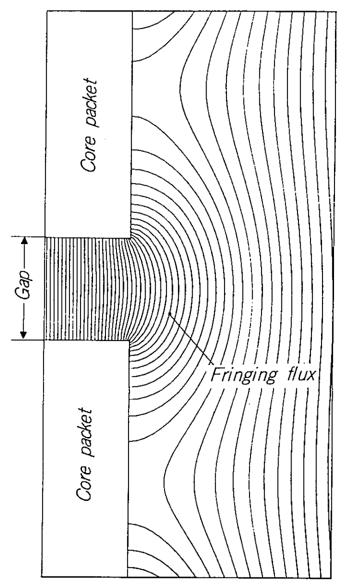

Fig. 4 Fringing flux distribution

III. DEVELOPMENT OF RADIALLY LAMINATED CORE TYPE SHUNT REACTOR

1. Features of radially laminated core

As described in the Chapter II above, the gapped-core type allows the reactor to be smaller in the dimensions and lighter in the weight in comparison with the air-core type.

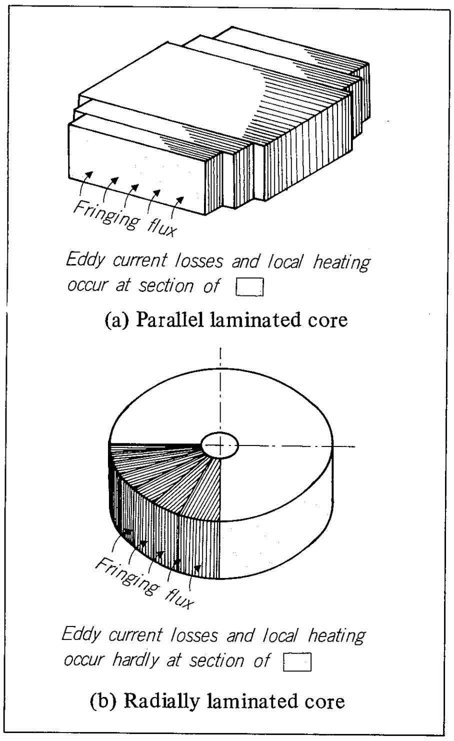

Fig. 5 Construction of core packet and fringing flux

When the conventionally well known parallel laminated core is used, however, eddy current losses and local heating occur due to the fringing flux which intrudes into the lamination plane of the silicon steel plate in the right angle as shown in *Fig. 5-(a)*, and for this reason, it has been said that the gapped-cord type which uses the parallel laminated cor packet is not suited to a large power reactor.

While, in case of the radially laminated core, the fringing flux entirely comes in and out toward the thickness direction of the silicon steel plates as shown in *Fig. 5-(b)*, because the silicon steel plates are laminated radially. Therefore, eddy current losses occurred on the core can be suppressed greatly and local heating can be prevented. Further, in case of a large power shunt reactor, when it is necessary to take a long total gap length, almost no problems due to the fringing flux occur even if a gap length is increased per position.

Table 1 Comparison between air-core type and gapped-core type

Item \ Type		Air-core type	Gapped-core type (Radially laminated core type)
Loss	(%)	100	85
Noise	(dB)	80	75
Total weight	(t)	298 (100%)	256 (86%)
Transport dimension	(m)	9.5 x 3.0 x 4.2	10.4 x 3.1 x 3.9

Note: Comparison was made with three-phase, 275 kV, 200 MVA shunt reactor.

Table 1 shows comparisons for losses, noises, weights and transporting dimensions between an air-core type 275 kV 200 MVA shunt reactor and a gapped-core type same power shunt reactor which uses a radially laminated core. As It is obvious from this table, the gapped-core type using radially laminated core is better in the loss, noise, weight and dimensions.

Perceiving the above described matters, Fuji Electric proceeded the development to employ the radially laminated iron core for a large power shunt reactor.

2. Construction of radially laminated core and manufacturing technique

Fig. 6 shows how a radially laminated core packet looks like. Silicon steel plates having several different widths are laminated radially, the circumference is tightened with glass wind tape after assembling the silicon steel plates in a circular shape, resin is impregnated into the core packet and thus, it is constructed to a single unit by hardening the resin. It may differ depending on the outer diameter of a core packet, number of used silicon steel plates is 4000 to 5000. The radially laminated core packet differs from the conventional laminated cores and the cross-section is a complete circle. Therefore, the space factor is high and the packet can be made small.

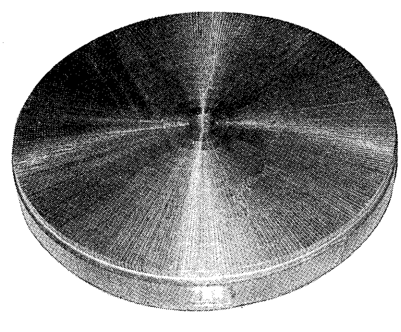

Fig. 6 Radially laminated core packet

When developing the core packet manufacturing techniques, the following three were major problems.

(1) Selection of suitable resin.

(2) To impregnate resin into gaps between the individual steel plates perfectly and to provide them with a sufficient adhesion.

(3) To prevent crack due to shrinkage of the resin during heat-hardening after impregnating resin into the layers.

To solve these problems, compression tests and thermal tests were repeated on the core packets manufactured for trials, further, long hour electric-charge tests were conducted, and extremely rigid core packets which are free from crack and steel plate deviations were completed. In addition, adhesive life tests had been conducted as acceleration test, and it has been confirmed that the adhesive life is long enough against the expected 30 year life of the shunt reactor for which the core packets are to be used.

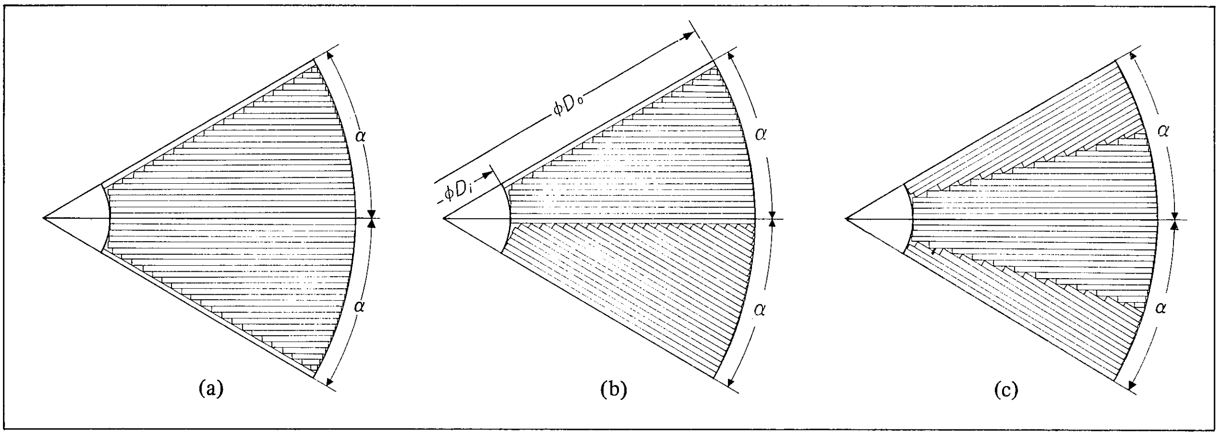

Fig. 7 Methods to laminated silicon steel plates of the radially laminates core packet

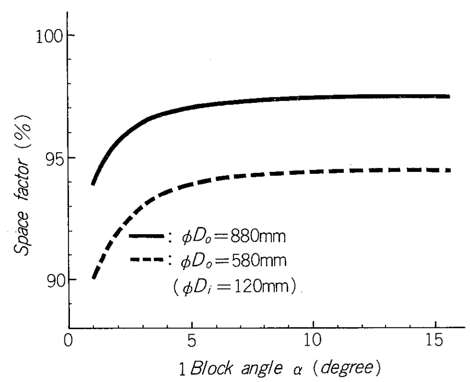

Fig. 8 Relation between 1 block angle α and space factor

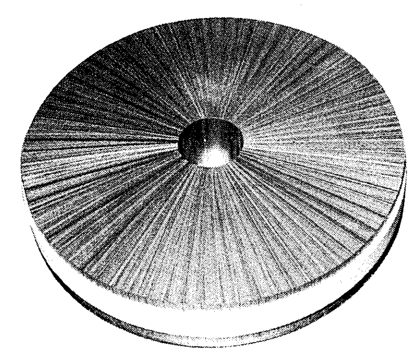

Fig. 10 High space factor type radially laminated core packet

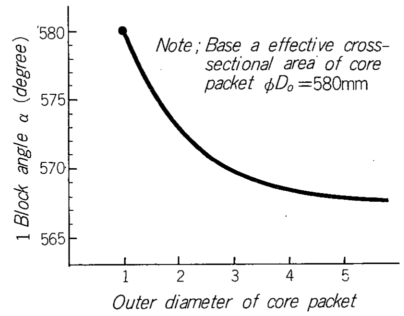

Fig. 9 Relation between outer diameter of core packet having a fixed effective cross-sectional area and 1 block angle α

3. Improvement of space factor of core packet

To reduce dimensions and weight of the gapped-core type reactor using a radially laminated core, improvement of space factor of the core packet is an important subject.

For methods to laminate silicon steel plates of the core packet, there is a method to further improve space factor as shown in *Fig. 7* in addition to the method shown in *Fig. 6*. Using the silicon steel plate laminiting method shown in *Fig. 7-(b)* as an example, relation of space factor against one block angle α is shown in *Fig. 8*, and changes of outer diameter of core packet having a fixed effective cross-sectional area against one block angle α are shown in *Fig. 9*. With these examples, it can be understood that space factor of a core packet can be improved and outer diameter can be reduced by selecting a pertinent one block angle α. *Fig. 10* shows how the core packet manufactured by the method shown in *Fig. 7-(b)* looks like.

4. Selection of optimum gap size

For both the magnetic flux value and fringing range toward the radius direction, fringing flux generated in a gap portion increases in proportion to the gap size, causing eddy current losses and local heating on the core packet and winding. For this reason, gap size must be decided very carefully. Particularly, in the case of a large power reactor, selection of an optimum gap size is an important subject of the design because gap size per position is large.

In the case of a radially laminated core, the fringing flux comes into and out from the core toward the thickness direction of the silicon steel plates. Therefore, even if a comparatively large gap size is selected, various problems due to fringing flux do not occur as described above. However, for the winding, expansions of fringing toward the radius directions are problems. For example, when a large gap size is selected, the fringing flux reaches even the

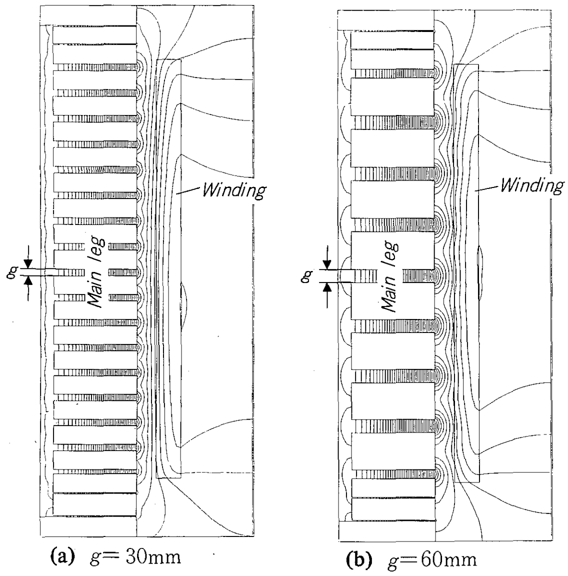

Fig. 11 An example of magnetic field mapping of radially laminated core type reactor

winding and disturbs magnetic flux within the winding, causing a local heating and eddy current loss in the winding. On the other hand, the gap between the core and winding is decided based on the insulation class of the winding, and for this reason, the optimum gap size must be decided by taking the insulation class into considerations.

For relationships between gap size and fringing flux, *Fig. 11* shows an example of magnetic field mapping. It can be understood from this figure that the winding is almost not affected when gap length is 30 mm, but the winding is somewhat affected when gap length is 60 mm.

Further, it is also important to reduce eddy current losses in the core and winding by adequately controlling magnetic flux distribution and by finely adjusting gap arrangements in both the inside and outside of the winding.

IV. CHARACTERISTICS OF A 500/$\sqrt{3}$ kV 80/3 MVA RADIALLY LAMINATED CORE TYPE SHUNT REACTOR

Fuji Electric recently manufactured 18 units single phase 500/$\sqrt{3}$ kV 80/3 MVA radially laminated core type shunt reactors. The test results are reported as follows.

The specifications are shown in *Table 2*, the construction of the core is shown in *Fig. 12*, and the appearance during testing is shown in *Fig. 13*.

1. Measurement of reactance

Reactances are obtained through precise magnetic field analysis (for example, *Fig. 11*) by the use of a computer. The calculated value of the reactance obtained through the magnetic field analysis well agrees with the actually measured value, and fluctuations against the mean values

Table 2 Specifications of shunt reactor

Item	Specifications
Type & Rated frequency	Outdoor use Single-phase, 50 Hz
Rated power	80/3 MVA (Continuous)
Rated voltage	500/$\sqrt{3}$ kV (105% maximum system voltage)
Insulation class	Line : BIL 1550 kV Neutral : BIL 550 kV
Cooling system	ONAN
Noise	75 dB
Connection	Star (Bank)
Standard	IEC-289

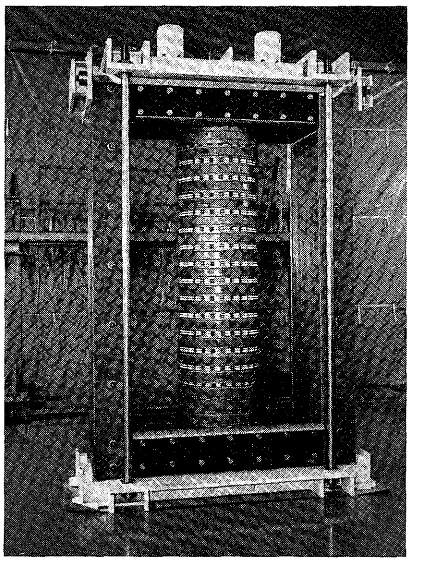

Fig. 12 Construction of the core

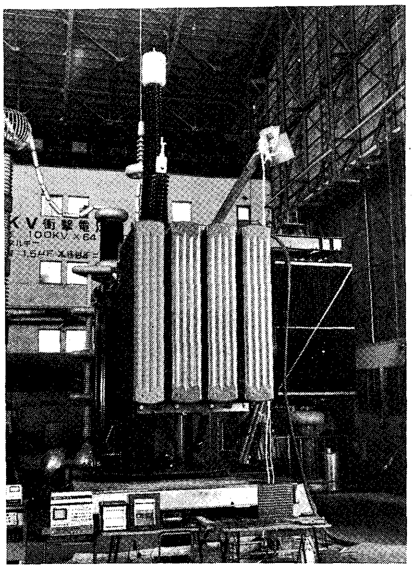

Fig. 13 Appearance during testing

were within 1%.

Fig. 14 shows results of the actual measurements of relationship between voltage and current.

2. Measurement of loss

Results of loss measurements (75 °C conversion at each applied voltage) are shown in *Fig. 15*. In comparison with the values estimated on a parallel laminated core type shunt reactor, the losses are 15 to 30% lower. (Ratio of Fuji Electric)

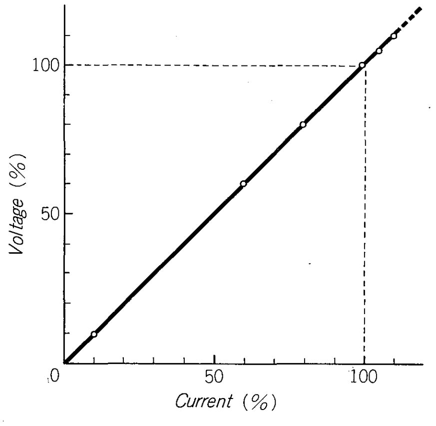

Fig. 14 Relation between voltage and current

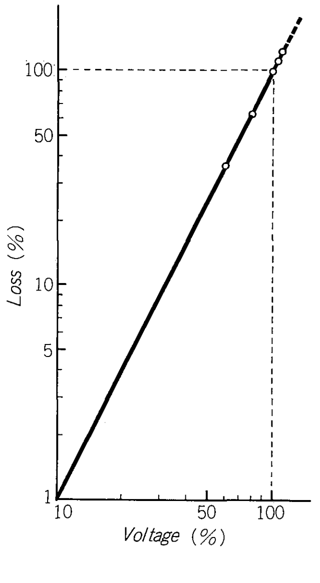

Fig. 15 Relation between loss and voltage

Table 3 Temperature rise test results

(°C)

Temperature rise \ Voltage	100%	105%
Oil (maximum)	42	46
Oil (mean)	36	40
Winding	49	54
Temperature rise of winding against oil temperature rise (mean value)	13	14

3. Temperature rise test

Table 3 shows the results of the temperature rise tests. The results sufficiently satisfy the standards, and local heating portion where gas is produced from the insulation mateiral and oil was not recognized.

4. Long-time temperature rise test

Long-time temperature rise tests and gas analysis in oil were conducted in the pattern shown in the *Fig. 16*. As the result, no abnormal occurrence was recognized at all. Further, during the tests, temperature distribution on the tank wall at each applied voltage was measured by a thermal imager probeye (*Fig. 17*). The maximum temperature is about equivalent to the maximum oil temperature, and no local heating was recognized.

5. Noise and vibration characteristics

In the case of a gapped-core type, vibrations of the shunt reactor occur mainly due to magnetic attraction force of the core gap, while in the case of an air-core type, mainly due to magnetic attraction force between the winding and yokes located the top and bottom of the winding. To reduce the vibrations, a pertinent magnetic flux density is selected, ceramic spacers having the longitudial elasticity equivalent to or higher than the core packet and having no secular change are used for the gaps, and the overall core is tightened toward the axial direction.

Fig. 18 shows the noise measurement results and *Fig.*

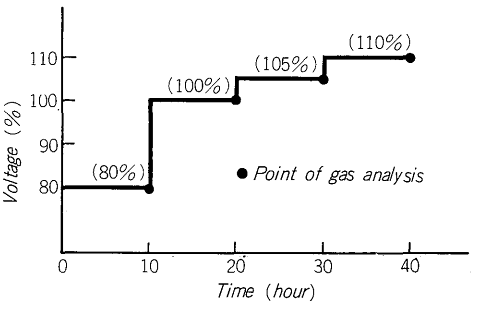

Fig. 16 Long-time temperature rise test

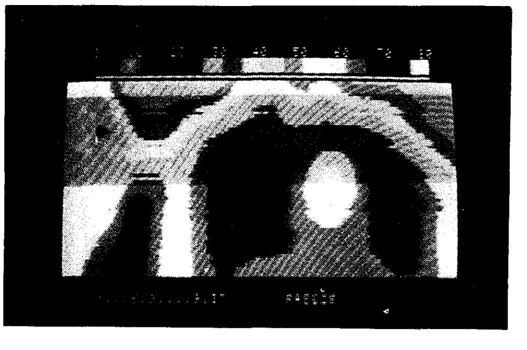

Fig. 17 An example of temperature distribution on the reactor tank wall by a thermal imager probeye

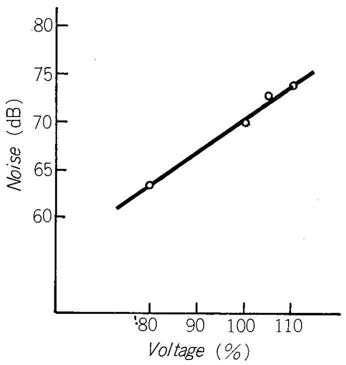

Fig. 18 Noise test results

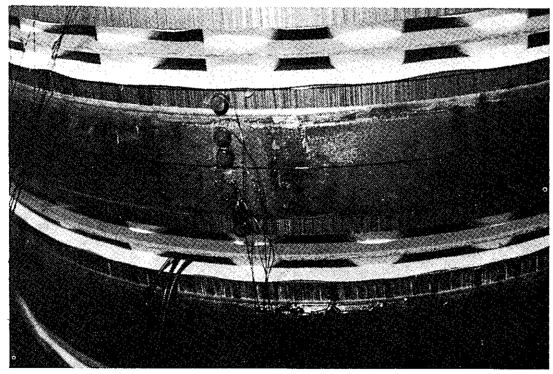

Fig. 20 Search coil for magnetic flux measurements

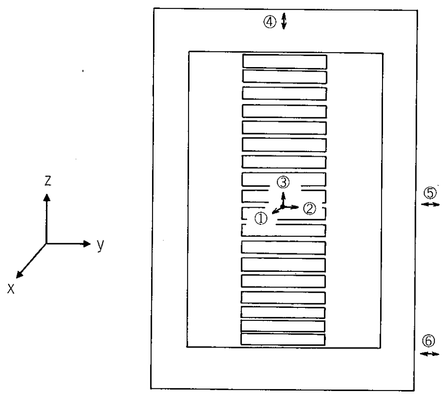

Position No.	Measured position	Amplitude (μm) (single amplitude)
①	Main leg (x-axis)	10
②	Main leg (y-axis)	3.6
③	Main leg (z-axis)	12
④	Upper yoke (z-axis)	6.5
⑤	Side pass (y-axis)	10
⑥	Side pass (y-axis)	2.6

(at 100% Voltage)

(a) Each part of core

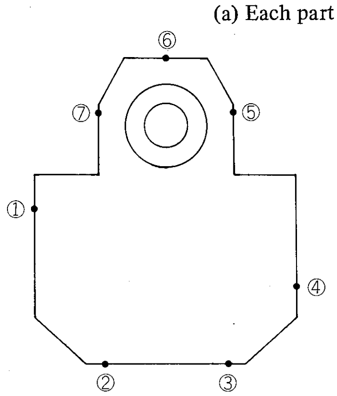

Position No.	Amplitude (μm) (single amplitude)
①	20
②	1.1
③	1.9
④	4.2
⑤	1.7
⑥	1.5
⑦	0.8

(at 100% Voltage)

(b) Each part of tank wall

Fig. 19 Oscillation test results

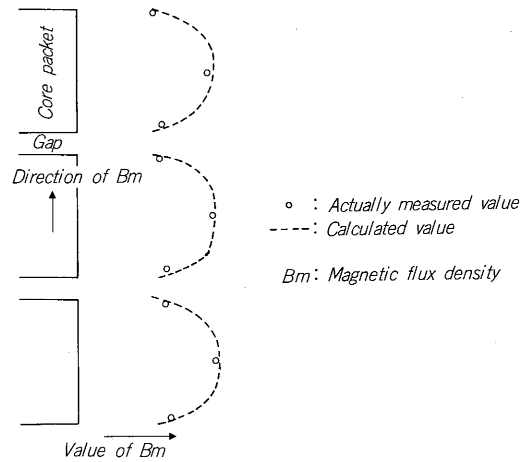

Fig. 21 Magnetic flux density distribution in main core

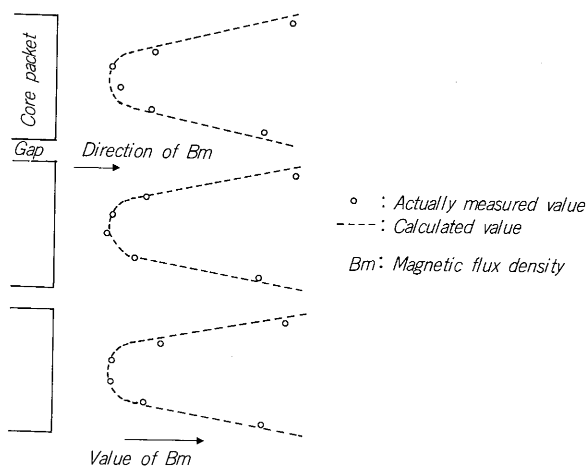

Fig. 22 Fringing magnetic flux density distribution at gap

19 shows the vibration measurement results. In comparison with the value estimated on a parallel laminated core type, the noise was 4 to 6 dB lower.

6. Measurement of magnetic flux density at each internal part

Search coils were installed on about 200 positions of a core (*Fig. 20*), magnetic flux densities were measured inside

Table 4 Typical manufacturing example of shunt reactor

Customer	The Tokyo Electric Power Co., Inc., Japan	CTM/AyEE, Argentina	PUB, Singapore
Phase	three-phase	single-phase	three-phase
Rated frequency (Hz)	50	50	50
Rated voltage (kV)	275	$500/\sqrt{3}$	230
Rated power (MVA)	150	140/3 120/3 70/3 50/3	100 50
Cooling system	OFWF	ONAN	ONAN
Quantity	2	7 6 6 30	1 2
Delivery year	1979	1978 ~ 1981	1979 ~ 1980
Appearance	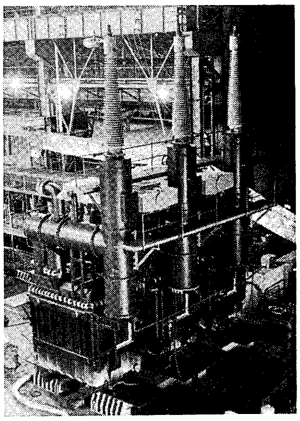	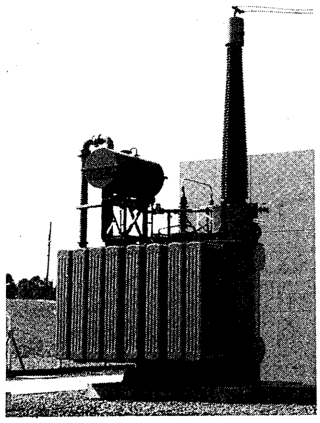	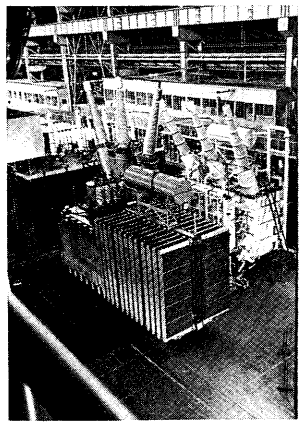
Note	divided-three-phase type underground substation use	Above picture shows 50/3 MVA reactor.	Above picture shows 100 MVA reactor.

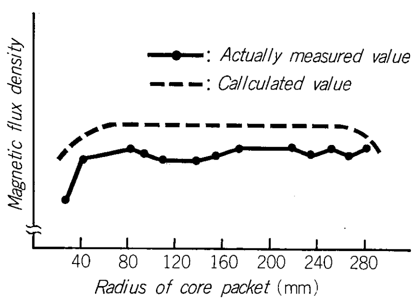

Fig. 23 Magnetic flux density distribution in gap

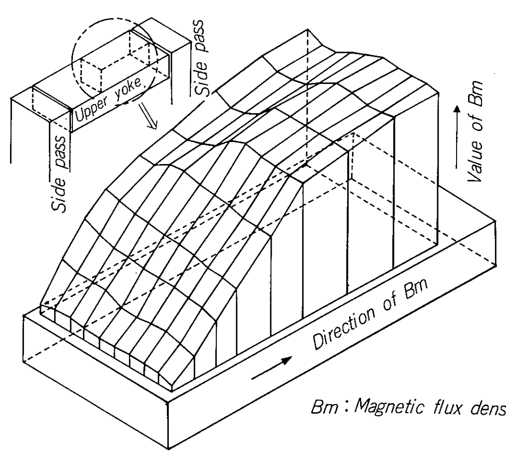

Fig. 24 Magnetic flux density distribution in upper yoke

the main core, circumference of the core packet, main leg gap and inside of the upper yoke, and the measured values were compared with the results of the magnetic field analysis by the use of a computer. For all values, the calculated values well agree with the actually measured values, and satisfactory results could be obtained.

Fig. 21 shows magnetic flux density distribution in main core, *Fig. 22* shows fringing magnetic flux density distribution of gap, *Fig. 23* shows magnetic flux density distribution in gap, and *Fig. 24* shows magnetic flux density distribution in upper yoke.

7. Others

In addition to the above introduced tests, temperature rise tests for the individual internal parts, harmonic content analyses of voltage and current, compression and thermal tests of the core packet, etc. were conducted, and for all, satisfactory results could be obtained.

Especially, for the temperature rise tests for the internal parts, a measuring instrument using a non-inductive optical fiber (with which temperatures can be measured precisely and directly even at an electrically charged portion and under electro magnetic inductive noise) was used.

As the results of comparison with the results of measurements using a thermocouple and thermoplate, it has been confirmed that the measuring method using the optical fiber has a sufficiently practical performance.

V. SHUNT REACTOR MANUFACTURING EXAMPLES

Before reaching the developments of radially laminated core type shunt reactors, Fuji Electric has manufactured and delivered many Extra high voltage large power shunt reactors. *Table 4* shows the typical manufacturing examples. Moreover, at present, Fuji Electric is planning to design a 275 kV 200 MVA shunt reactor.

VI. CONCLUSION

For the recent technological trends of shunt reactors, the basic constructions of the radially laminated core developed to cope with the requirements for reductions of loss, noise and dimensions were introduced, and results of tests conducted on the recently completed and delivered 500 kV bank power 80 MVA radially laminated core type shunt reactor were outlined.

Considering that the radially laminated core type shunt reactors will be used for wider applications because of the various features, Fuji Electric has estaglished a policy to manufacture radially laminated core type shunt reactors as the standard products up to the large power class that can presently be presumed.